Journal of Advanced Research 16 (2019) 55–65

Contents lists available at ScienceDirect

Journal of Advanced Research

journal homepage: www.elsevier.com/locate/jare

Original Article

Optical properties and colorimetry of gelatine gels prepared in different saline solutions

Mohammad A.F. Basha

Physics Department, Faculty of Science, Cairo University, P.O. Box 12613, Giza, Egypt

HIGHLIGHTS

- Gelatine gels were prepared by gelation in solutions of transition metal chlorides.
- The properties of the resulting gels depend on the salt type and concentration.
- SDT values for the gelatine gels were correlated to the solutions' concentrations.
- The gelatine gels exhibited significant improvement in their thermal stability.
- FTIR spectroscopy indicated a loss in the helical structure of the gels.

GRAPHICAL ABSTRACT

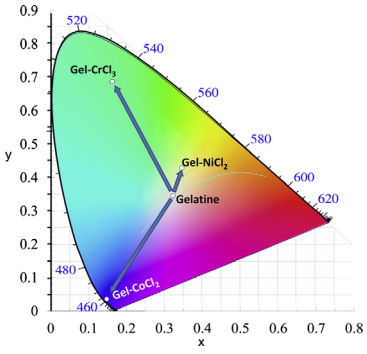

ARTICLE INFO

Article history:
Received 29 August 2018
Revised 9 December 2018
Accepted 10 December 2018
Available online 13 December 2018

Keywords:
Gelatine
Transition metals
Fourier transform infrared spectroscopy
Thermogravimetric analysis
Optical properties
Colour parameters

ABSTRACT

Gelatine has been widely used in many multidisciplinary research fields due to its biocompatibility. Using saline solutions in the gelation of gelatine allows for new properties to be incorporated into the prepared gels. This study examined the optical and colour properties of gelatine gels prepared in saline solutions, containing three different metal chlorides ($NiCl_2{\cdot}6H_2O$, $CoCl_2{\cdot}6H_2O$, and $CrCl_3{\cdot}6H_2O$) with concentrations of up to 50%, to prepare three groups of gels. FTIR spectroscopy indicated a loss in the helical structure of the metal-containing gelatine gels, and a shift in the amide bands towards lower wavenumbers. From the thermogravimetric analysis (TGA), the starting degradation temperatures (SDTs) of the prepared gelatine gels were found to be correlated to the concentration of the gelling solutions. All SDTs were above 250 °C, making these gels suitable for standing temperatures beyond the daily range. UV–vis spectroscopy showed that d-d transitions were responsible for the colour properties of the metal-containing gelatine gels. It is concluded that the studied properties and the measured parameters were found to depend on both salt type and concentration. With the current findings, the prepared gels can be used as optical thermometers, colour-selective corner cube retroreflectors, laser components, and coatings for OLEDs.

Introduction

Gelatine is a polypeptide biopolymer that consists of proteins and peptides resulting from the partial reduction of protein during the hydrolysis process of collagen. Gelatine is soluble in hot water and most polar solvents. At room temperature, gelatine is a translucent, colourless brittle material that has an α-helical structure. However, some of gelatine's physical properties, mainly its elastic properties, are highly sensitive to temperature variations [1,2]. The presence of different functional groups in gelatine's structure, such as carboxyl and amino groups, provides gelatine the unique ability to complex with other materials [3,4]. To date, scientists have managed to alter many gelatine properties by

Peer review under responsibility of Cairo University.
E-mail address: mafbasha@gmail.com

https://doi.org/10.1016/j.jare.2018.12.002
2090-1232/

adding other biomolecules and metal salts for different purposes [5,6]. Because of its biocompatibility, non-toxicity and low cost, gelatine has been used in many industries for various applications, including the food, pharmaceutical and medical industries [7–9]. The production of a non (or low)-degradable gelatine that can withstand temperature variations and ultraviolet radiation is desirable for widening the applications of gelatine to other medical and industrial fields, including those pertaining to photography, protective media, optical coatings, edible optics, eye-contact lenses, ocular tissue engineering, colour controllers and lacquered gelatine; one sample application is Wratten filters, which enable the selective transmission of certain wavelengths [1,10–13]. Such gels can also be used as filters for colour-selective corner cube retroreflectors and white OLEDs [11,14,15].

For the application of gelatine in the field of optics, it is essential to study gelatine's optical and colour properties. The physical gelation of gelatine in saline solutions using different metal chlorides has been studied from the perspective of changes in the triple helical structure, changes in gelling temperature and the rheological and elastic properties of gelatine gels [1,2,16,17]. It is believed that the strength of gelatine gels decreases with the addition of chloride salts, while the gelling temperature increases with salt concentration [1].

The current study is aiming to examine the improvements in the optical and colour properties of gelatine gels prepared by gelation in solutions containing different transition metal salts with different concentrations. The metal salts used in this work were nickel (II) chloride hexahydrate ($NiCl_2{\cdot}6H_2O$, green), cobalt (II) chloride hexahydrate ($CoCl_2{\cdot}6H_2O$, purple) and chromium (III) chloride hexahydrate ($CrCl_3{\cdot}6H_2O$, dark green). These salts were chosen for their strong colour effects and ease of solubility in distilled water near room temperature [18,19]. Moreover, the metal chlorides used in this work are multivalent salts that contain additional counterions that may increase the crosslinking effect [7,20,21].

Although small amounts of these metal salts are considered harmless, caution should be taken in their use in applications that involve direct inhalation or ingestion. Cobalt plays a biologically essential role as a metal constituent of vitamin B12; however, excessive exposure has been shown to induce various adverse health effects [22]. Although Ni is considered an essential element in microorganisms, plants, and animals and is a constituent of enzymes and proteins, excessive Ni affects the photosynthetic functions of higher plants, causes acute and chronic diseases in humans and reduces soil fertility [23,24]. Little information has been reported on the toxicity of trivalent Cr. Available data show little or no toxicity associated with Cr(III) at levels reported on a per kg basis [25]. Cr(III) is also used as a nutrient supplement [26]. Independent studies should be conducted to determine the toxicity of the gelatine gels used in this research based on the levels of the metal salts present in the materials.

Herein, the thermal properties and degradation of the prepared samples are discussed in the TGA section in terms of the thermodynamic parameters. The macrostructure of gelatine gels is discussed in the Fourier transform infrared (FTIR) spectroscopy section in terms of the vibrational modes. Finally, discussions of the optical and colour properties are provided in the UV–visible spectroscopy and colour parameters sections, respectively.

Experimental

Materials

The gelatine used in this research is a type B food-grade powder (average MW 45000, bloom no. 175) supplied by E. Merck (Darmstadt, Germany). The gelatine's maximum limit of ash impurity was 2.0%, and its grain size was less than 800 μm. Type B gelatine usually has an isoelectric point (IEP) between 4.8 and 5.4 [27]. Hydrated $NiCl_2{\cdot}6H_2O$, $CoCl_2{\cdot}6H_2O$ and $CrCl_3{\cdot}6H_2O$ of 99.9% purity were supplied by Strem Chemicals Inc. (Newburyport, MA, USA). Samples were classified into three groups, each corresponding to one salt type. The salts were added in different weight concentrations with the help of a micro-analytical balance (Sartorius). The salt concentrations in the gelling solutions were 5%, 10%, 15%, 20%, 30% and 50% (see Table 1). The gelation process was performed for all samples under the same conditions as follows: Weighted amounts of gelatine and salts were dissolved separately in 100 mL of double-distilled water. The solutions were sterilized using an HL-320 tabletop autoclave at 121 °C for 15 min. The pressure inside the autoclave was then released, and the containers of the solutions were removed. Gelatine solutions were then mixed with the salt solutions of the corresponding weight percentage. The mixtures were further sterilized in a 65 °C water bath for 15 min until the gelatine and salt had thoroughly dissolved. The resulting solutions were poured into glass dishes with an area of 25 cm^2 and stored for a few hours at 4 °C. The dishes were then incubated for 30 to 45 min at 37 °C until a fine coating of thickness ~1 mm was formed.

Methodology

Thermal stability was investigated for the prepared gelatine gels using a computerized thermogravimetric analysis (TGA) instrument (TA-50) manufactured by Shimadzu Corporation (Kyoto, Japan). TGA measurements were performed in a nitrogen atmosphere under a flow rate of 0.5 mL/sec. A heating rate of 10 K/min was used for all samples over the temperature range from room temperature (~35 °C) to 600 °C. Fourier transform infrared (FTIR) spectra were measured for the prepared gelatine gels using a Shimadzu FTIR-8400S spectrophotometer (Shimadzu Corporation, Tokyo, Japan) over the wavenumber range 400 to 4000 cm^{-1} (wavelength 2.5 to 25 μm). UV–visible absorption and transmission spectra were obtained for the prepared gelatine gels using a Perkin-Elmer 4-B spectrophotometer (Perkin-Elmer, Waltham, MA, USA) over the wavelength range of 200 to 800 nm.

Results and discussion

Thermogravimetric analysis (TGA)

Fig. 1 shows the TGA curves and their derivative curves (DrTGA) for all gelatine gels. The TGA curves of all gelatine gels exhibit three steps of degradation. The first step in the TGA curve represents a steep degradation phase from room temperature to T ~ 160 °C. During this phase, pure gelatine loses approximately 14.5% of its mass due to the evaporation of residual water absorbed from the atmosphere, which contributes significantly to the weight of gelatine. The second step of the TGA curve represents a shallow phase that starts from T ~ 160 °C and extends to ~240 °C (~241.6 °C for pure gelatine gels). This phase is characterized by a negligible loss in mass, which indicates negligible or no disintegration. It is worth mentioning that the upper temperature limit for that phase is far beyond the daily temperature range. The third degradation step is the steepest among the three phases, which starts at 245 °C and represents the main decomposition regime. This degradation phase is mainly associated with the disintegration and partial breaking of intermolecular structure due to endothermic hydrolysis and oxidation reactions [28]. Exothermic reactions occur after the pyrolysis of the derived collagen, leading to a mass loss of 85% at the end of the final degradation step. The remaining mass at 700 °C (973 K) was approximately 0.063% of the

Table 1
The codes used in this research for the gel samples and their corresponding salt type and concentration according to the weight percentages.

Sample group	Saline solution concentration						
	5%	10%	15%	20%	30%	40%	50%
Gelatine + $CoCl_2$	Gel-Co5	Gel-Co10	Gel-Co15	Gel-Co20	Gel-Co30	Gel-Co40	Gel-Co50
Gelatine + $NiCl_2$	Gel-Ni5	Gel-Ni10	Gel-Ni15	Gel-Ni20	Gel-Ni30	Gel-Ni40	Gel-Ni50
Gelatine + $CrCl_3$	Gel-Cr5	Gel-Cr10	Gel-Cr15	Gel-Cr20	Gel-Cr30	Gel-Cr40	Gel-Cr50

original, most of which was ash formed by carbon residues. The remaining mass of the gels in the saline solutions was approximately 0.030% of the original mass.

Fig. 1 (a) shows that the starting decomposition temperature (SDT) for the main degradation phase increased with salt concentration, indicating an improvement in thermal stability. The Dr-TGA curves in Fig. 1 (b) show that the rate of decomposition during the main degradation phase for the Gel-Co gelatine gels increased with salt concentration. Moreover, Gel-Co20, Gel-Ni5 and Gel-Cr10 exhibited the maximum decomposition rate during their main degradation phase compared with the other concentrations in their corresponding groups. The percentage mass loss and the starting decomposition temperature for all gelatine gels are presented in Table 2.

The thermodynamic parameters of the gelatine gels were examined by employing the Coats–Redfern equation [29]:

$$\ln\frac{-\ln(1-\alpha)}{T^2} = -\frac{E^{\#}}{RT} + \ln\frac{AR}{\theta E^{\#}}\left[1-\frac{2RT}{E^{\#}}\right], \quad (1)$$

where A is a pre-exponential constant, θ is the heating rate, R is the universal gas constant (8.3145 J K^{-1} mol^{-1}), and α is the fractional decomposition at temperature T [29,30]. The relation in Eq. (1) was plotted for all the gelatine gels as shown in Fig. 2. The Coats–Redfern equation was fitted by a straight line to find parameter A. Thermodynamic parameters such as the activation energy ($E^{\#}$), enthalpy ($\Delta H^{\#}$), entropy ($\Delta S^{\#}$) and Gibbs free energy ($\Delta G^{\#}$) were calculated based on the laws of thermodynamics as follows:

$$\Delta H^{\#} = E^{\#} - RT, \quad (2)$$

$$\Delta S^{\#} = 2.303[\log\frac{Ah}{kT}]R, \quad (3)$$

$$\Delta G^{\#} = \Delta H^{\#} - T\Delta S^{\#}, \quad (4)$$

where k is Boltzmann's constant and h is Planck's constants. The Coats–Redfern relation for pure gelatine is shown in Fig. 2 (a). The calculated thermodynamic parameters for pure gelatine during the first degradation phase are $E^{\#} \sim 26.340$ kJ/mole, $\Delta H^{\#} \sim 23.430$ kJ/mole, $\Delta S^{\#} \sim -231.459$ J/mole and $\Delta G^{\#} \sim 104.440$ kJ/mole, whereas for the main degradation phase, $E^{\#} \sim 81.222$ kJ/mole, $\Delta H^{\#} \sim 76.250$ kJ/mole, $\Delta S^{\#} \sim -143.265$ J/mole and $\Delta G^{\#} \sim 161.922$ kJ/mole. The parameter values for all the gelatine gels are presented in Table 2.

A negative entropy value is a measure of orderness. Small values of the thermodynamic activation parameters for the first degradation phase relative to those for the main degradation phase indicate relatively lower thermal motion, higher order and a more stable structure for materials heated to temperatures of up to ~250 °C.

Fourier transform infrared (FTIR) spectroscopy

An interaction between electromagnetic radiation and a molecule inside a material can only occur if there is a moving electrical charge associated with the molecule. Such movement is always the case when the molecule has either a variable or an inducible dipole moment (IR-active). In molecules with oscillations symmetric to the centre of symmetry, no changes in the dipole moment occur (IR-inactive). However, such "forbidden" vibrations are often Raman-active. In the case of polyatomic molecules, the fundamental vibrations are superimposed. Accordingly, a series of absorption bands that must be interpreted arises.

Fig. 3 presents the FTIR spectra of pure gelatine and the gelatine gels Gel-Co30, Gel-Ni30 and Gel-Cr30. The FTIR spectrum for pure gelatine in Fig. 3 consists of a broad amide *A* band at 3577 cm^{-1}, a C═O stretching band in the amide *I* band at 1693 cm^{-1}, an NH bending band at 1575 cm^{-1} and a CH_2 bending band at 1575 cm^{-1} in the amide *II* band and an amide *III* NH bending band and a C—O stretching band at 1268 cm^{-1} and 1096 cm^{-1}, respectively [31]. It is believed that the triple helical structure content of gelatine is closely related to the mechanical and physical properties of gelatine gels [32]. During the gelation process, the polymer structure changes from random separate coils to helical chains cross-linked by flexible peptide chains. The main interaction mechanisms involved in the conformations of gelatine chains are hydrogen bonds, hydrophobic effects and electrostatic interactions [1]. However, due to the large ionic strength of saline solutions, the addition of salt will cause a decrease in the electrostatic interactions due to electrostatic shielding, leaving the hydrogen bond mechanism as the main noncovalent source of stability for the helix structure. Moreover, the excess amount of multivalent counter ions in polyelectrolyte solutions will increase the probability of crosslinking or complexation between the multivalent counter ions and polyelectrolyte solution [7,21]. The FTIR spectra in Fig. 3 shows significant changes in the relative intensities and positions of the main bands, which depended on the type of salt. The transmittance relative intensities were measured for each spectrum relative to the baseline within the same spectrum. The baseline was considered the horizontal line that passes through the maximum point of the spectrum; this point was found to be approximately the same for all spectra at a transmittance value of ~98.5. The decrease in the relative intensities of the amide *I*, *II* and *III* bands for the metal-containing gelatine gels indicates an increase in disorder, which is associated with loss of the helix structure [33]. The intensity of the amide *III* band has been associated with the triple helical structure of the collagen-like content of the partly regenerated collagen, and a lower relative intensity of that band indicates that gelatine gels host fewer intermolecular interactions [31]. The broader amide *A* band observed in the FTIR spectrum of the Gel-Co30 gelatine gel indicates a higher degree of molecular order, suggesting that gelatine gels of the Gel-Co group may have contained a significant number of intermolecular crosslinks of covalent bonds that survived the gelation process. Additionally, the inset in Fig. 3 shows a shift in the positions of the amide *I* C═O stretching band and the amide *II* NH bending band towards lower wavenumbers, which is dependent on the type of saline solution. These changes confirm the modification of the helical structure of gelatine, which is sensitive to experimental conditions such as temperature variations, the type of solvent used and ionic strength [2,17,34]. The degradation of the triple helix structure associated with the collagen-like content of the partly regenerated collagen during the gelling process was found to decrease the Bloom index,

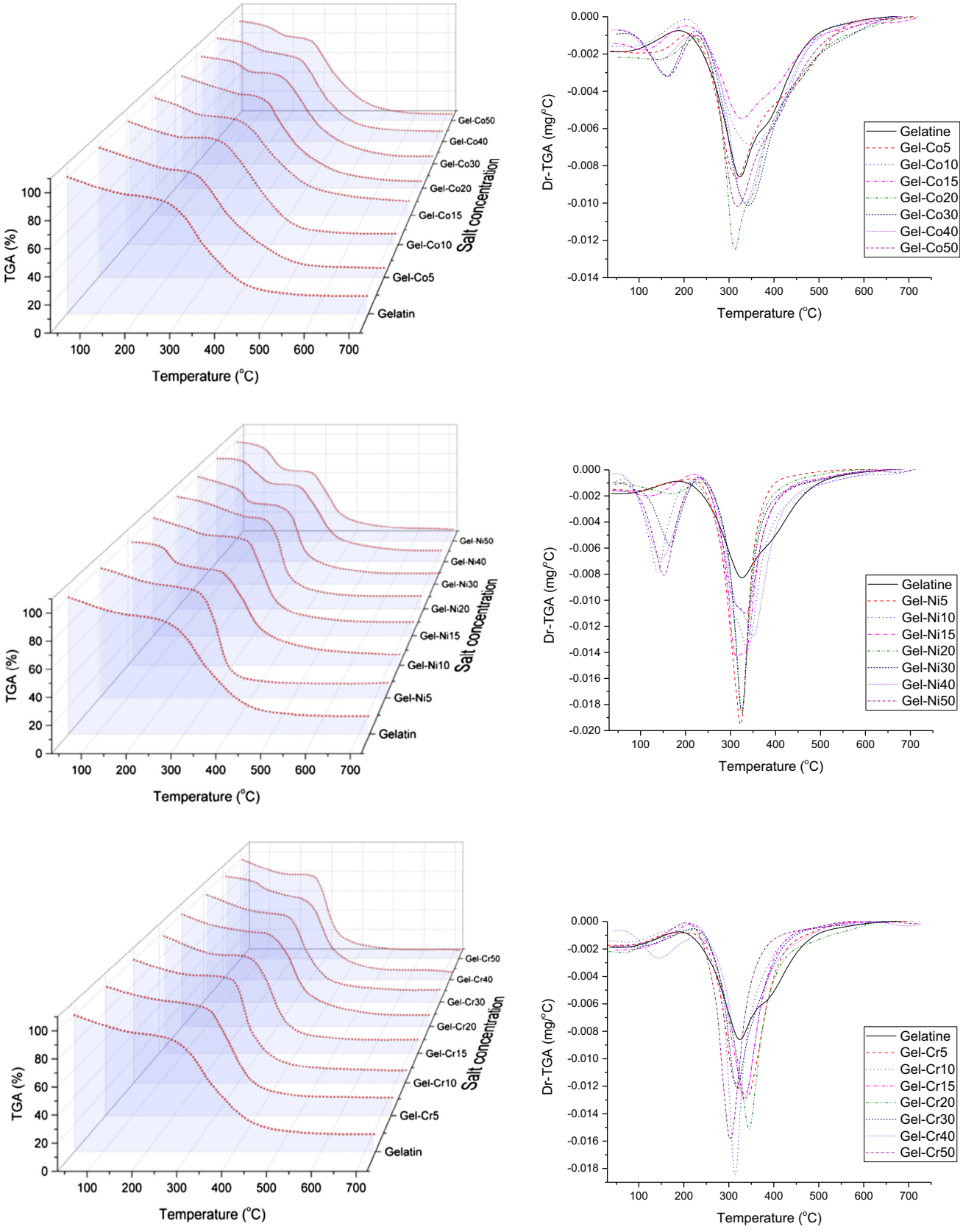

Fig. 1. TGA results and the corresponding differential curves for all gel groups; Gel-Co, Gel-Ni and Gel-Cr.

Table 2
The percentage mass loss, the starting decomposition temperatures (SDTs) and the thermodynamic parameters (activation energy $E^{\#}$, entropy $\Delta S^{\#}$, enthalpy $\Delta H^{\#}$ and Gibbs free energy $\Delta G^{\#}$) for the gels under study.

Sample	Temperature (K)		Mass loss	SDT	Thermodynamical parameters			
	Start	End	%	°C	$E^{\#}$ (kJ/mole)	$\Delta S^{\#}$ (J/K/mole)	$\Delta H^{\#}$ (kJ/mole)	$\Delta G^{\#}$ (kJ/mole)
Gel-Co5	300	435	13.8		20.970	−268.893	17.914	116.732
	560	900	85.9	245.8	21.857	−257.365	15.788	203.664
Gel-Co10	300	435	13.6		27.662	−257.991	24.607	119.418
	560	900	86.2	247.0	23.721	−252.378	17.651	201.888
Gel-Co15	300	435	15.7		16.795	−277.098	13.740	115.573
	560	900	87.0	248.7	26.119	−246.078	20.050	199.687
Gel-Co20	300	435	12.1		19.437	−272.230	16.382	116.426
	560	900	87.7	250.4	29.400	−240.282	23.331	198.736
Gel-Co30	300	435	9.3		24.750	−263.498	21.695	118.531
	560	900	88.5	252.7	35.619	−229.324	29.550	196.957
Gel-Co40	300	435	11.1		22.518	−266.701	19.463	117.476
	560	900	88.7	254.4	30.738	−240.635	24.669	200.333
Gel-Co50	300	435	8.2		22.550	−266.482	19.495	117.427
	560	900	91.6	257.3	33.115	−238.356	27.046	201.046
Gel-Ni5	300	435	13.3		55.602	−201.205	52.547	126.490
	560	900	86.7	276.1	22.643	−255.750	16.574	203.272
Gel-Ni10	300	435	18.8		34.293	−242.596	31.238	120.391
	560	900	81.0	285.9	44.530	−203.740	38.461	187.192
Gel-Ni15	300	435	14.5		48.891	−216.065	45.836	125.240
	560	900	85.3	300.2	22.501	−256.374	16.432	203.585
Gel-Ni20	300	435	12.4		51.838	−209.906	48.783	125.924
	560	900	87.4	315.6	24.469	−254.003	18.400	203.822
Gel-Ni30	300	435	14.5		39.523	−231.636	36.468	121.594
	560	900	85.3	323.5	22.641	−256.770	16.572	204.014
Gel-Ni40	300	435	16.7		36.876	−238.273	33.820	121.385
	560	900	83.3	343.5	60.928	−162.007	54.859	173.124
Gel-Ni50	300	435	21.6		31.768	−245.495	28.712	118.932
	560	900	78.2	353.1	36.998	−221.616	30.929	192.708
Gel-Cr5	300	435	12.4		54.578	−206.845	51.523	127.539
	560	900	87.4	259.0	18.676	−264.877	12.606	205.967
Gel-Cr10	300	435	12.7		71.940	−174.366	68.885	132.964
	560	900	87.0	263.6	21.027	−259.003	14.958	204.030
Gel-Cr15	300	435	15.9		59.029	−198.215	55.974	128.818
	560	900	83.8	269.9	24.876	−248.751	18.807	200.395
Gel-Cr20	300	435	14.1		50.986	−214.581	47.930	126.789
	560	900	85.7	275.6	20.211	−259.985	14.141	203.930
Gel-Cr30	300	435	15.4		55.123	−204.700	52.067	127.295
	560	900	84.3	278.5	23.747	−251.554	17.678	201.313
Gel-Cr40	300	435	12.9		53.503	−208.896	50.447	127.216
	560	900	86.8	285.4	29.399	−245.051	23.329	202.216
Gel-Cr50	300	435	15.0		61.455	−189.590	58.400	128.074
	560	900	84.7	291.6	22.923	−253.216	16.854	201.701

hence decreasing the gel strength [32,35]. Moreover, the shift of the amide I C═O and amide II NH bands to lower wavenumbers for the metal-containing gelatine gels implies a decrease in their gel strength when explained in terms of the local oscillator approach, in which an intermolecular bond can be approximated as a spring characterized by a force constant determining its strength [36,37]. In this case, the wavenumber of the oscillator is correlated with the force constant, and hence, a decrease in wavenumber due to the addition of chloride salts can be attributed to a decrease in gel strength.

UV–visible spectroscopy

UV–visible spectroscopy is a spectroscopic method that uses electromagnetic waves of ultraviolet (UV) and visible (VIS) light to study the electronic structure of materials. It is believed that a material's electronic structure, the location of its energy levels and electronic transitions between them are among the factors that affect colour properties [38].

The UV–visible spectra obtained for the metal-containing gelatine gels are shown in Figs. 4–6. The changes in the spectroscopic properties according to metal ion type stem from the partly filled d subshells in these metals, which lead to their chromophoric properties caused by d-d transitions and charge transfer transitions such as π-to-π* transitions that take place at longer wavelengths. UV light can provide information about the absorbing wavelength of a molecule, its structure and its colour. The larger the number of conjugated double bonds is, the longer the wavelength of absorbed light will be. If the energy of π-to-π* transitions lies within the range of visible light, the colour of the molecule is complementary to that of the absorbed light. For the Gel-Co group of gels, as shown in Fig. 4 (a), two bands appeared in the visible parts of each spectrum. The peaks of the bands were centred around wavelengths 530 and 635 nm, which correspond to the transitions $^4A_{2g} - {}^4T_{lg}$ and $^4T_{lg}(P) - {}^4T_{lg}$ of the Co^{2+} ion, respectively. The spectra of the Gel-Ni group of gels shown in Fig. 5 (a) indicate two main peaks characteristic of the hexaaquo ion $[Ni(H_2O)_6]^{2+}$. The first peak is centred at approximately 400 nm and was assigned to the $^3A_{2g} - {}^3T_{lg}$ transition, whereas the second peak is a broad one centred at approximately 722 nm and was assigned to the $^3T_{2g} - {}^3T_{lg}$ transition. For the Gel-Cr group of gels, as shown in Fig. 6 (a), the transitions were due to complex ions consisting of the hexaaquo ion $[Cr\ (H_2O)_6]^{3+}$ mixed with the aquo ions $[Cr(H_2O)_5C1]^{2+}$ and $[Cr(H_2O)_4C1_2]^{+}$ [39]. The spectra were

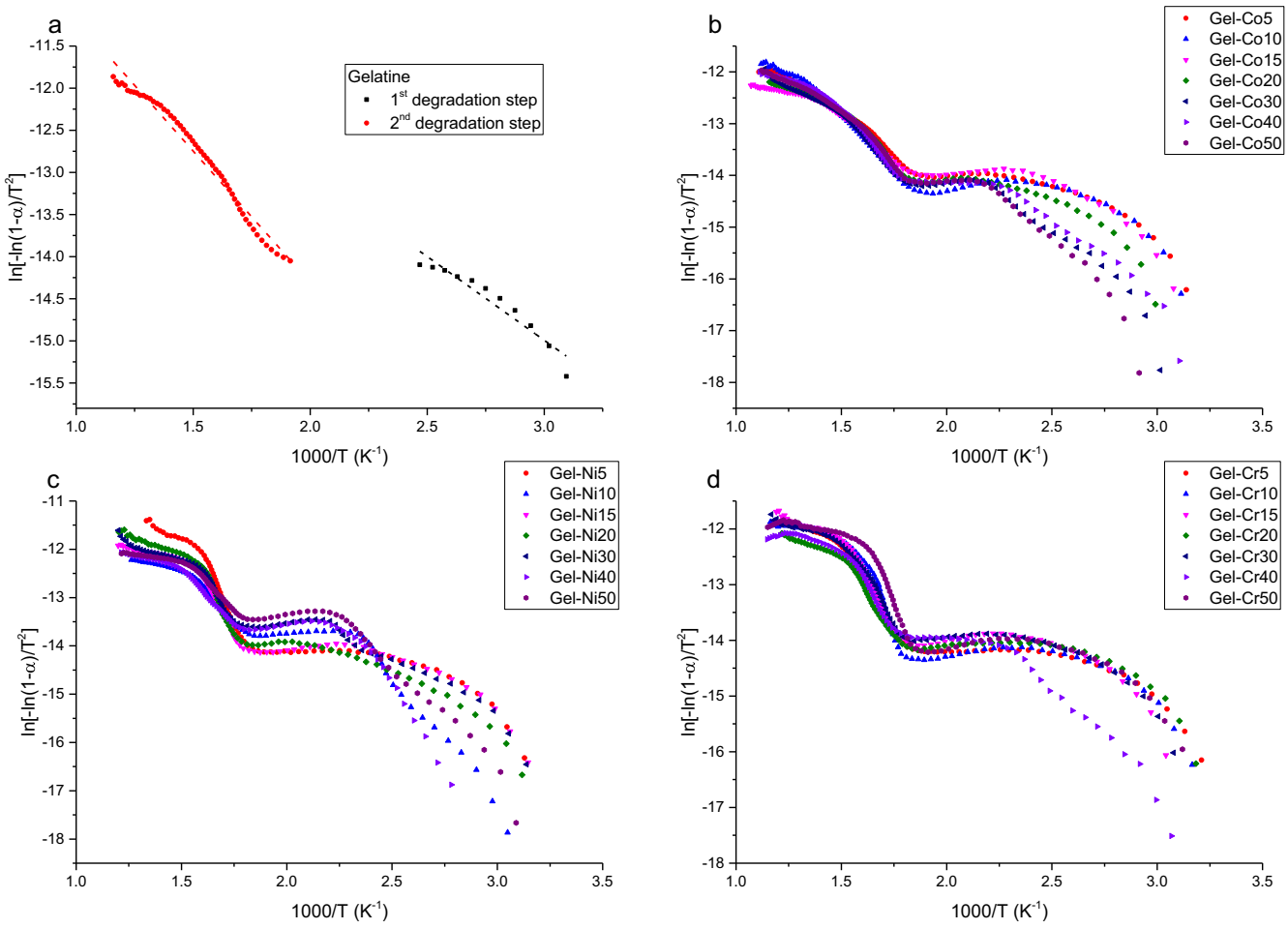

Fig. 2. The Coats–Redfern relation for gelatine prepared in pure aqueous solution (a) and gels prepared in $CoCl_2$ (b), $NiCl_2$ (c) and $CrCl_3$ (d) solutions.

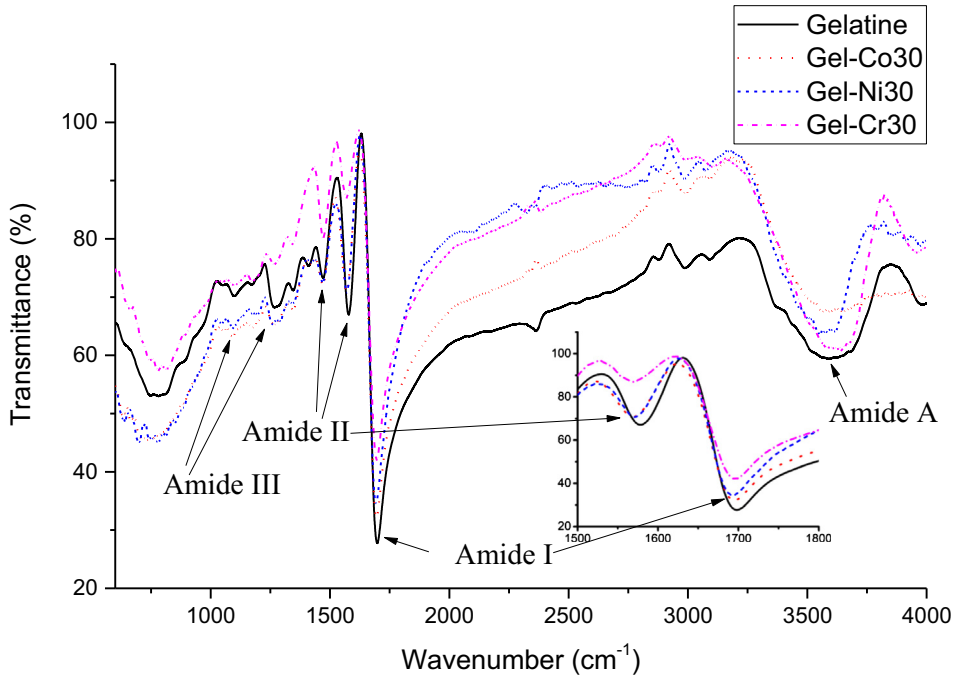

Fig. 3. FTIR spectra of gelatine gel prepared in aqueous solution and the gels Gel-Co30, Gel-Ni30 and Gel-Cr30. The inset is a magnification of the amide I C=O stretching band and the amide II NH bending band that indicates changes in these bands depending on the type of solvent.

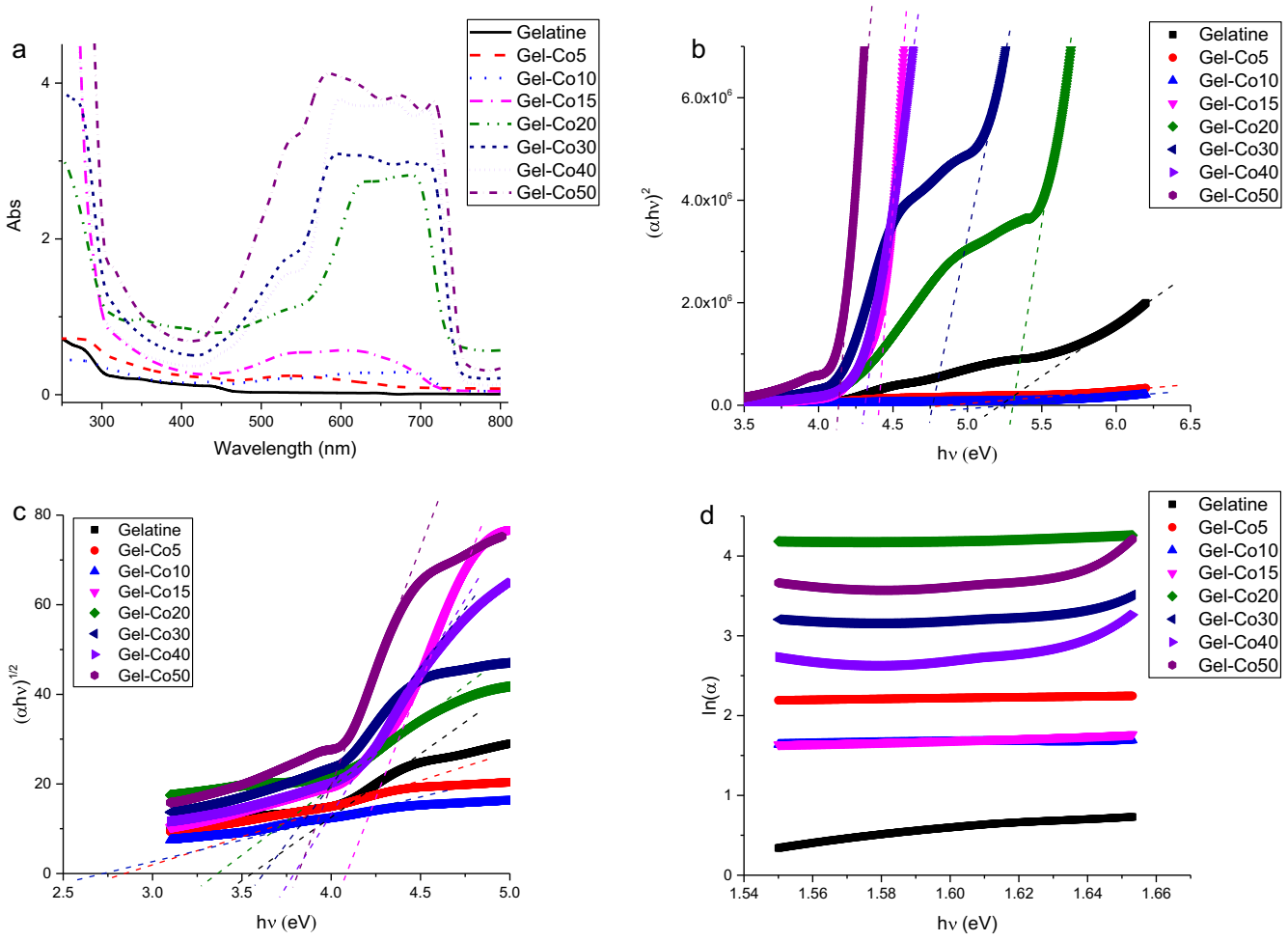

Fig. 4. UV–vis spectroscopy results for the Gel-Co group of gels: (a) UV–vis spectrum, (b) Tauc plots of $(\alpha h\upsilon)^2$ vs. $h\upsilon$ for the allowed direct transition, (c) Tauc plots of $(\alpha\, h\upsilon)^{1/2}$ vs. $h\upsilon$ for the allowed indirect transition and (d) plots of $\ln(\alpha)$ vs. $h\upsilon$ from the Urbach equation.

characterized by two main peaks centred at approximately 430 and 590 nm assigned to the transitions $^4T_{2g} - {}^4A_{2g}$ and $^4T_{1g} - {}^4A_{2g}$, respectively.

To raise an electron from the highest occupied molecular orbital (HOMO) to the lowest unoccupied molecular orbital (LUMO), the energy of the absorbed photon must exactly match the energy difference between the two energy levels. The wavelength of the absorbed light can be calculated according to the formula $E = h\upsilon = \frac{hc}{\lambda}$, where E is the energy of the absorbed light, h is Planck's constant, c is the speed of light and υ and λ are the frequency and wavelength of the electromagnetic wave, respectively.

The band gaps between the transition levels can be calculated from the Tauc plots, which plot $(\alpha h\upsilon)^{1/r}$ versus $h\upsilon$. Here, α is the absorption coefficient and is directly determined from the optical absorption data provided by the UV–vis spectrometer using the relation $\alpha = \frac{A}{d}$, where A is the absorbance and d is the thickness of the gelatine gel. The exponent r used in the Tauc plots can assume four values: $r = 1/2$ for direct allowed transitions, $r = 3/2$ for direct forbidden transitions, $r = 2$ for indirect allowed transitions and $r = 3$ for indirect forbidden transitions. Only the allowed transitions were considered in this research; thus, the Tauc relations using $r = 1/2$ for direct transitions and $r = 2$ for indirect transitions were plotted as shown in Figs. 4–6 for the Gel-Co, Gel-Ni and Gel-Cr groups, respectively. The linear part of the curve is extrapolated to intersect with the x-axis at the band gap value. For pure gelatine, the value of the direct allowed band gap is 3.556 eV, whereas the value of the indirect allowed band gap is 5.217 eV. The values of the direct band gaps E_d and the indirect band gaps E_{in} for the gelatine gels are shown in Table 3.

Along the absorption coefficient curve and near the optical band edge, there is an exponential part called the Urbach tail. The exponential tail appears because of the existence of localized states that extend into the band gap. In the range of low photon energy, the spectral dependence of the absorption coefficient (α) and photon energy (E) is given by the equation $\alpha = \alpha_o exp\left(\frac{E}{E_U}\right)$, where α_o is a constant and E_U denotes the energy of the band tail. Taking the natural logarithm of the two sides of the equation, one can obtain a straight line representing the relation between $\ln(\alpha)$ and the incident photon energy ($E = h\upsilon$), as shown in Figs. 4–6, for the Gel-Co, Gel-Ni and Gel-Cr groups, respectively. The band tail energy, or Urbach energy (E_U), can be obtained from the slope of the straight line. The Urbach energy for pure gelatine was found to be 0.312 eV. The Urbach energies for the metal-containing gelatine gels are listed in Table 3.

Colour parameters

The method of trichromaticity colorimetry enables determination of the colour trajectory in the Commission Internationale de l'Eclairage (CIE) 1931 colour space, where each colour corresponds to the appropriate and unique point in that space whose positional parameters are related to the tristimulus values X, Y, and Z [38].

The CIE standard colour system was defined by the International Commission on Illumination to establish a relationship

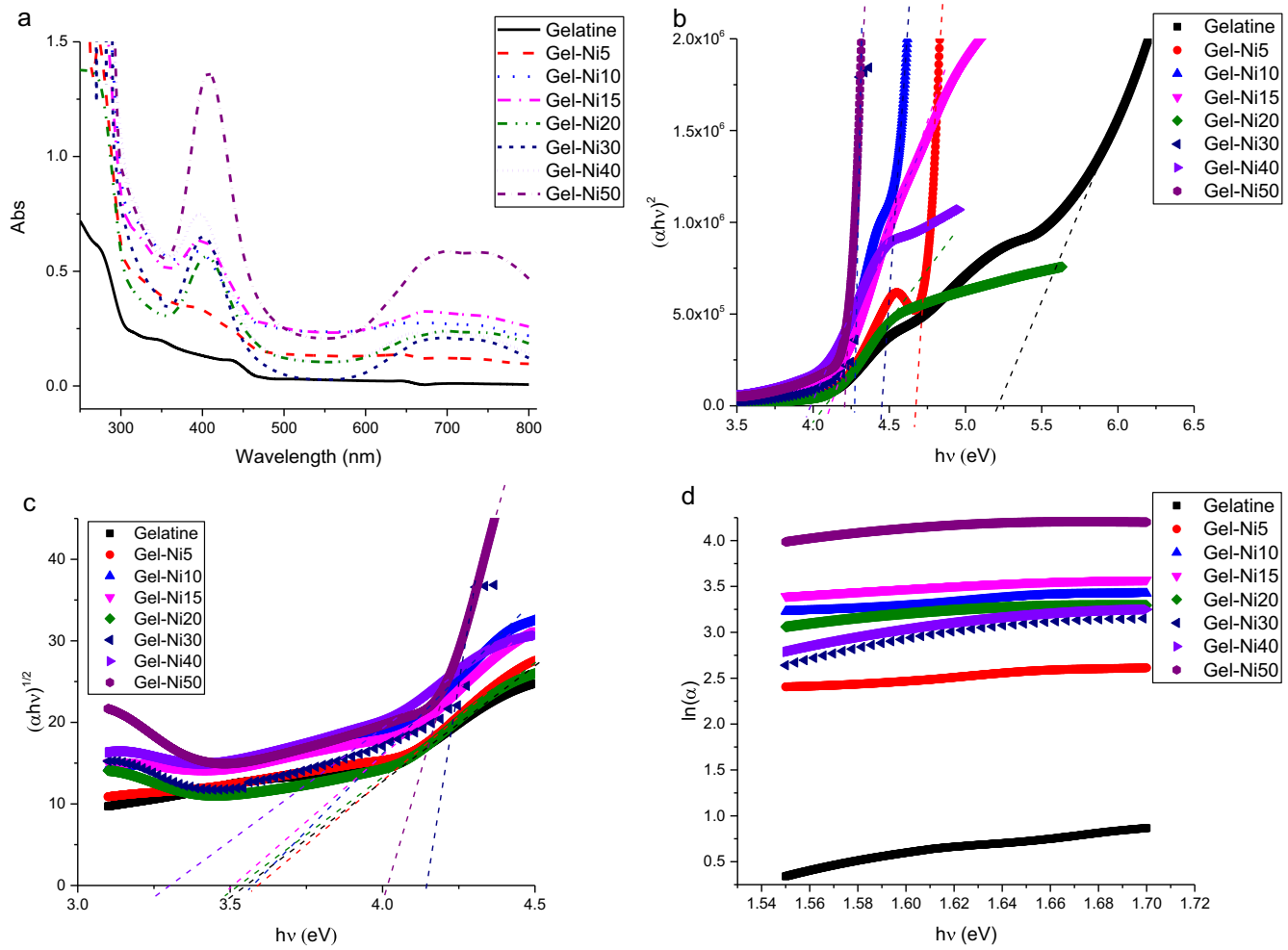

Fig. 5. UV–vis spectroscopy results for the Gel-Ni group of gels: (a) UV–vis spectrum, (b) Tauc plots of $(\alpha h\upsilon)^2$ vs. $h\upsilon$ for the allowed direct transition, (c) Tauc plots of $(\alpha\, h\upsilon)^{1/2}$ vs. $h\upsilon$ for the allowed indirect transition and (d) plots of $\ln(\alpha)$ vs. $h\upsilon$ from the Urbach equation.

between human colour perception and the physical causes of colour appeal using the colour space coordinates. The three basic values of the colour space coordinates X, Y and Z are called tristimulus values. Each colour can be identified by such a triplet consisting of the normalized tristimulus values x, y and z. Thus, the term tristimulus system is customary for the CIE standard system.

The tristimulus values for a colour can be calculated from the spectral reflectance values $R(\lambda)$ using the following integrals over the visible wavelength range (380 to 780 nm):

$$X = \frac{K}{N}\int_{380}^{780} R(\lambda)I(\lambda)\,\bar{x}(\lambda)d\lambda$$

$$Y = \frac{K}{N}\int_{380}^{780} R(\lambda)I(\lambda)\,\bar{y}\,(\lambda)d\lambda$$

$$\text{and} Z = \frac{K}{N}\int_{380}^{780} R(\lambda)I(\lambda)\,\bar{z}\,(\lambda)d\lambda$$

where $N = \int_{380}^{780} I(\lambda)\,\bar{z}\,(\lambda)d\lambda$, K is a scaling factor (usually 100) and $I(\lambda)$ is the spectral power distribution of the spectrometer lamp. $\bar{x}(\lambda)$, $\bar{y}(\lambda)$ and $\bar{z}(\lambda)$ are called the colour matching functions. The parameter Y is also a measure of the luminance of a colour.

The normalized tristimulus (chromaticity coordinates) values were calculated for the gelatine gels using the following equations:

$$x = \frac{X}{X+Y+Z}$$

$$y = \frac{Y}{X+Y+Z}$$

$$\text{and} z = \frac{Z}{X+Y+Z} = 1 - x - y$$

Fig. 7 represents the CIE chromaticity coordinate of the studied gelatine gels with respect to a white D65 reference source. The colour of the gelatine gels can be varied by changing the salt type and concentration. For the Gel-Co group of samples, as shown in Fig. 7 (a), the colour of the gelatine gels changed from near the white point towards the purplish blue with increasing $CoCl_2$ concentration. As shown in Fig. 7 (b), the increase in the $NiCl_2$ concentration led to a change in the colour of the gelatine gels towards the yellow-green region, whereas the change in colour for the Gel-Cr group, as shown in Fig. 7 (c), was found to be towards the green as the $CrCl_3$ concentration increased. The colours of the gelatine gels of the Gel-Co group were close to the Planckian locus, whereas the colours of the low-salt-concentration gelatine gels in the Gel-Ni and Gel-Cr groups were near the white region and possessed small colour gradients. The blackbody correlated colour temperature (CCT) can be calculated from the chromaticity coordi-

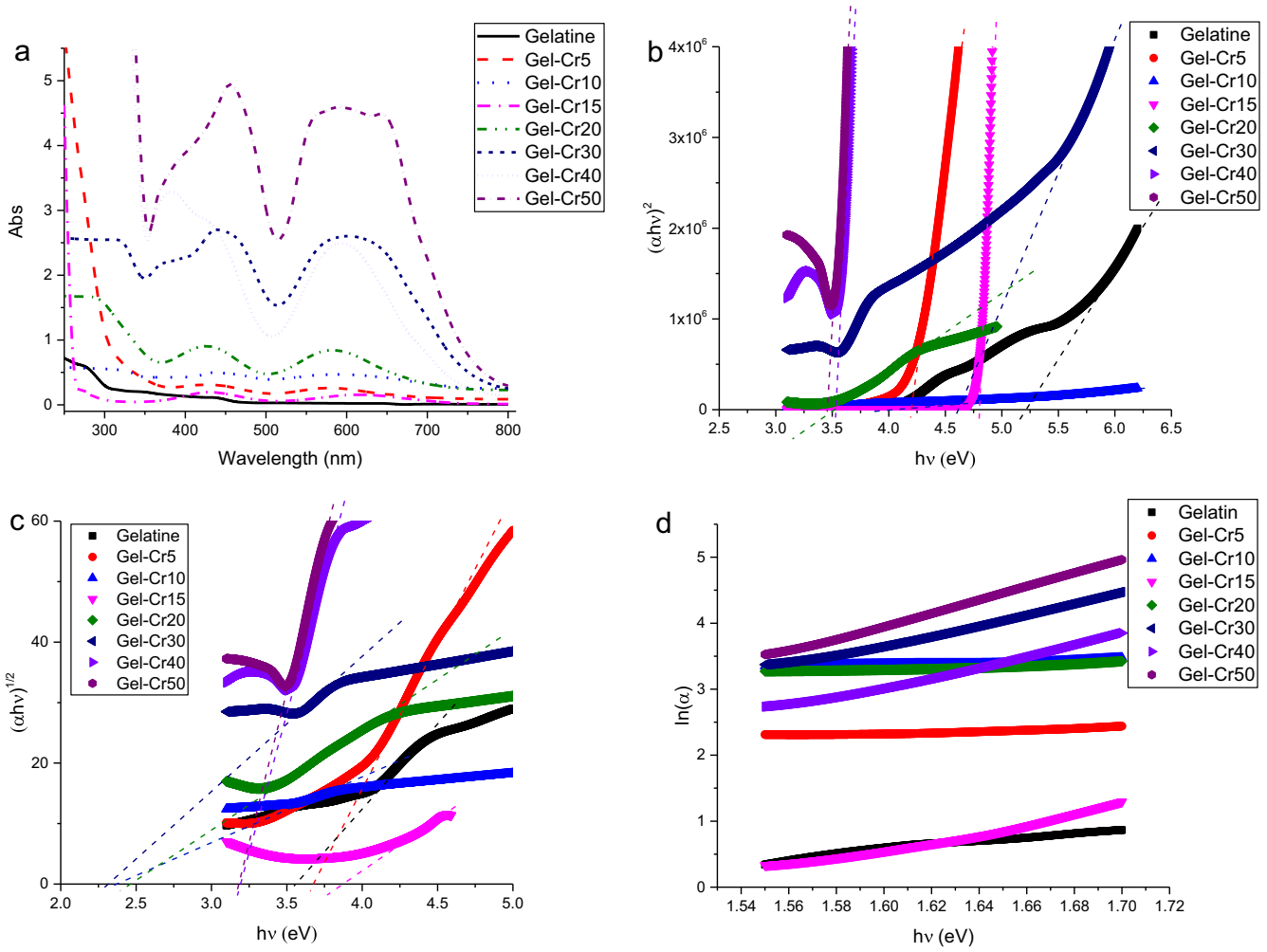

Fig. 6. UV–vis spectroscopy results for the Gel-Cr group of gels: (a) UV–vis spectrum, (b) Tauc plots of $(\alpha h\upsilon)^2$ vs. $h\upsilon$ for the allowed direct transition, (c) Tauc plots of $(\alpha\, h\upsilon)^{1/2}$ vs. $h\upsilon$ for the allowed indirect transition and (d) plots of $\ln(\alpha)$ vs. $h\upsilon$ from the Urbach equation.

Table 3
The values of the direct band gaps E_d, the indirect band gaps E_{in} and the Urbach energies E_U.

Sample	E_d (eV)	E_{in} (eV)	E_U (eV)
Gel-Co5	4.876	2.825	0.828
Gel-Co10	5.238	2.727	0.395
Gel-Co15	4.415	4.084	0.510
Gel-Co20	5.314	3.690	0.506
Gel-Co30	4.772	3.623	0.084
Gel-Co40	4.312	3.787	0.060
Gel-Co50	4.136	3.814	0.069
Gel-Ni5	4.675	3.591	0.609
Gel-Ni10	4.447	3.572	0.636
Gel-Ni15	4.112	3.510	0.791
Gel-Ni20	4.076	3.527	0.641
Gel-Ni30	4.271	4.143	0.291
Gel-Ni40	3.985	3.304	0.321
Gel-Ni50	4.203	4.015	0.712
Gel-Cr5	4.198	3.677	1.189
Gel-Cr10	3.986	2.370	1.527
Gel-Cr15	4.803	3.866	0.157
Gel-Cr20	3.534	2.465	1.085
Gel-Cr30	4.613	2.316	0.132
Gel-Cr40	3.537	3.194	0.131
Gel-Cr50	3.455	3.182	0.101

nates. Hue (H_{ue}) is another parameter perceived by people as a fundamental characteristic of colour. In colour theory, hue refers to the property according to which one distinguishes colour sensations, for example, red, yellow or green. A colour of the same hue can either vary in saturation, such as grey blue versus blue, or in brightness, for example pink versus red.

Chroma (C^*) describes the relative colour effect relative to the reference white, i.e., relative to the brightest point of a colour space. The chroma is suitable as a measurement value for conical colour spaces, for example, where it can be measured from the top. These systems are useful in the printing industry. The colour parameters obtained for the gelatine gels are presented in Table 4.

The differences in brightness (ΔL^*), red-green colour (ΔU^*) and yellow-blue (ΔV^*) colour were calculated with respect to the properties of the pure gelatine gel [40]. Table 4 shows that the gelatine gels of the Gel-Ni group became more greenish and more yellowish as the concentration of the gelling solution increased. Additionally, the chroma of all the gelatine gels tended to increase with concentration. Fig. 7 (d) and (e) show the change in brightness difference (ΔL^*) and CCT according to the concentrations of the gelation solution, respectively. For the Gel-Co and Gel-Cr groups, the brightness difference tended to decrease with increasing concentration, whereas the CCT value increased with concentration. For the Gel-Ni group, CCT tended to decrease with concentration.

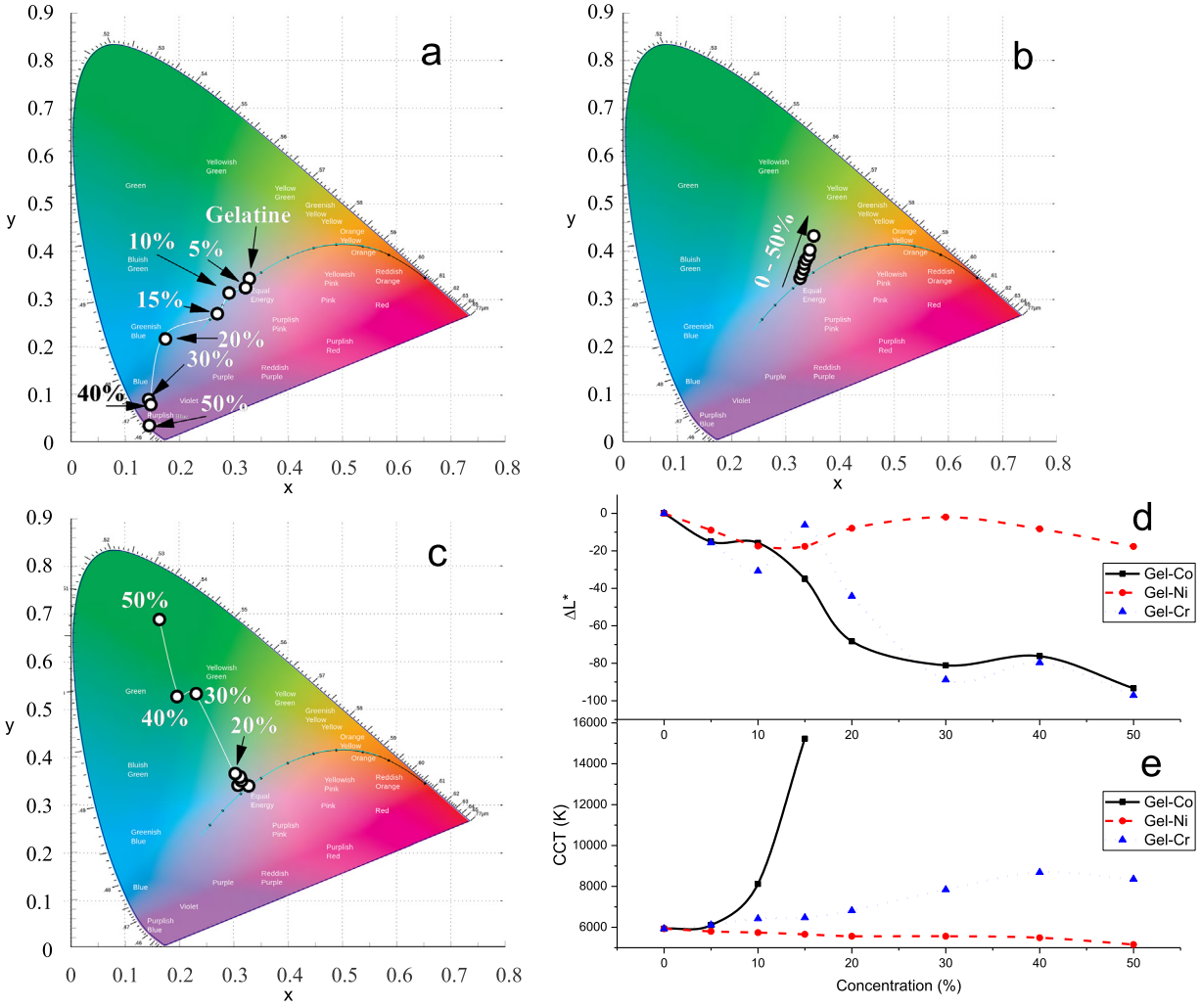

Fig. 7. Commission Internationale de l'Eclairage (CIE) 1931 colour space for (a) Gel-Co group of gels, (b) Gel-Ni group of gels and (c) Gel-Cr group of gels. (d) and (c) The dependences of brightness difference (ΔL^*) and CCT on solvent concentration, respectively.

Table 4
The difference in colour parameters (brightness ΔL^*, red-green ΔU^*, yellow-blue ΔV^* and chroma ΔC^*) calculated with respect to those of the gelatine gel prepared in pure aqueous solution. The blackbody correlated colour temperature (CCT) in Kelvin and hue (H_{ue}) for the gels under study.

Sample	ΔL^*	ΔU^*	ΔV^*	H_{ue}	ΔC^*	CCT (K)
Gel-Co5	−15.123	7.051	−13.958	159.996	15.638	6099.0
Gel-Co10	−15.748	−11.781	−24.526	51.630	27.209	8120.2
Gel-Co15	−35.061	−9.291	−49.747	78.025	50.607	15228.9
Gel-Co20	−68.285	−27.708	−46.854	53.392	54.434	–
Gel-Co30	−81.151	−9.394	−70.552	82.046	71.175	–
Gel-Co40	−76.201	−13.132	−85.334	80.785	86.339	–
Gel-Co50	−93.383	−1.570	−31.011	88.576	31.050	–
Gel-Ni5	−9.000	−0.739	3.183	91.350	3.268	5795.0
Gel-Ni10	−17.471	−3.154	6.205	83.105	6.961	5739.0
Gel-Ni15	−17.602	−4.266	9.882	81.308	10.764	5652.6
Gel-Ni20	−7.967	−6.915	18.207	78.690	19.476	5559.9
Gel-Ni30	−1.999	−10.136	23.916	75.450	25.975	5558.4
Gel-Ni40	−8.278	−8.268	22.476	77.870	41.400	5483.1
Gel-Ni50	−17.700	−13.670	39.078	75.880	4.136	5152.8
Gel-Cr5	−15.676	−4.199	−1.104	72.472	4.341	6113.1
Gel-Cr10	−30.789	−5.432	−5.984	49.013	8.082	6417.5
Gel-Cr15	−6.262	−13.356	1.631	45.804	13.455	6469.8
Gel-Cr20	−44.236	−15.903	0.055	36.705	15.903	6816.0
Gel-Cr30	−88.847	−12.018	−3.361	34.913	12.480	7840.4
Gel-Cr40	−79.685	−26.636	3.597	29.728	26.878	8686.2
Gel-Cr50	−97.132	−1.872	−10.441	35.016	10.607	8352.5

Conclusions

This research represents a study of the thermal, optical and colorimetric properties of gelatine gels prepared in different saline solutions containing the transition metal salts $NiCl_2{\cdot}6H_2O$, $CoCl_2{\cdot}6H_2O$ and $CrCl_3{\cdot}6H_2O$ The effect of salt concentration on the studied properties was considered, and the variables were compared within the same salt type for different concentrations and for the different salts, taking into account the properties of pure gelatine. A spectroscopic study utilizing FTIR was performed on the gelatine gels to investigate the nature of interactions between the salt ions and the gelatine functional groups. The results suggested the existence of crosslinking or complexation interactions either by direct linking of the ions to the gelatine bridge or by indirect effects on peptide folding by interacting with structurally linked water molecules. The results showed that the changes in the gelatine helical structure were highly sensitive to salt type and concentration. These changes had a direct effect on the structural and physical properties of the prepared gelatine gels. The results of FTIR and TGA indicated that the gel strength of the gelatine gels decreased due to the addition of chloride salts, whereas their thermal stability increased with salt concentration. UV–vis spectroscopy showed that the d-d transitions corresponding to the wavelengths in the visible region were responsible for the colour properties of the gelatine gels. The colours of the Gel-Co group were found to be near the Planckian locus region, and CCT steadily increased with $CoCl_2$ concentration. This sensitive dependence of the salt concentration on the CCT allows for these gels to be used as accurate optical thermometers (temperature sensors and transducers) in extreme temperature environments, such as the turbine inlet in jet engines, stationary gas turbine power plants and nuclear reactor plants. The gels of the Gel-Co group can also be used as filters for colour-selective corner cube retroreflectors, which can be applied in satellite communication, laser components and antennas. The colours of the Gel-Ni and Gel-Cr groups were found to be near the white region and possessed small colour gradients correlated to concentration. The gels of the Gel-Ni and Gel-Cr groups show promise for producing good-quality coatings and filters for white OLEDs. All studied physical properties and the calculated parameters were found to be highly sensitive to the salt concentrations.

Conflict of interest

The authors have declared no conflict of interest.

Compliance with Ethics Requirements

This article does not contain any studies with human or animal subjects.

References

[1] Qiao C, Zhang J, Ma X, Liu W, Liu Q. Effect of salt on the coil-helix transition of gelatine at early stages: Optical rotation, rheology and DSC studies. Int J Biol Macromol 2018;107:1074–9.
[2] Gornall JL, Terentjev EM. Helix–coil transition of gelatine: helical morphology and stability. Soft Matter 2008;4:544.
[3] Xu SW, Zheng JP, Tong L, De Yao K. Interaction of functional groups of gelatine and montmorillonite in nanocomposite. J Appl Polym Sci 2006;101:1556–61.
[4] Akhtar N, Shao H, Ai F, Guan Y, Peng Q, Zhang H, et al. Gelatine-polyethylenimine composite as a functional binder for highly stable lithium-sulfur batteries. Electrochim Acta 2018;282:758–66.
[5] Basha AF, Basha MA. Impact of neutron irradiation on the structural and optical properties of PVP/gelatine blends doped with dysprosium (III) chloride. J Appl Phys 2017;122:235104.
[6] Basha MA-F, Hassan MA. Structural and optical properties improvements of PVP/gelatine blends induced by neutron irradiation. Radiat Phys Chem 2018;146:47–54.
[7] Kaewruang P, Benjakul S, Prodpran T, Encarnacion AB, Nalinanon S. Impact of divalent salts and bovine gelatine on gel properties of phosphorylated gelatine from the skin of unicorn leatherjacket. LWT - Food Sci Technol 2014;55:477–82.
[8] Raghavendra GM, Jayaramudu T, Varaprasad K, Ramesh S, Raju KM. Microbial resistant nanocurcumin-gelatine-cellulose fibers for advanced medical applications. RSC Adv 2014;4:3494–501.
[9] Rose JB, Pacelli S, El Haj AJ, Dua HS, Hopkinson A, White LJ, et al. Gelatine-based materials in ocular tissue engineering. Materials (Basel) 2014;7:3106–35.
[10] Djabourov M. Architecture of gelatine gels. Contemp Phys 1988;29:273–97.
[11] Ahmed R, Yetisen AK, Yun SH, Butt H. Color-selective holographic retroreflector array for sensing applications. Light Sci Appl 2017;6:e16214.
[12] Wang X, Farrell G, Lewis E, Tian K, Yuan L, Wang P. A humidity sensor based on a single mode-side polished multimode-singlemode optical fibre structure coated with gelatine. J Light Technol 2017;35:4087–94.
[13] Knotts ME. Optics fun with gelatine. Opt Photonics News 1996;7:50.
[14] Kang X, Yang Y, Wang L, Wei S, Pan D. Warm white light emitting diodes with gelatine-coated $AgInS_2$/ZnS core/shell quantum dots. ACS Appl Mater Interfaces 2015;7:27713–9.
[15] Gong X, Ma W, Ostrowski JC, Bazan GC, Moses D, Heeger AJ. White electrophosphorescence from semiconducting polymer blends. Adv Mater 2004;16:615–9.
[16] Chatterjee S, Bohidar HB. Effect of cationic size on gelation temperature and properties of gelatine hydrogels. Int J Biol Macromol 2005;35:81–8.
[17] Sow LC, Yang H. Effects of salt and sugar addition on the physicochemical properties and nanostructure of fish gelatine. Food Hydrocoll 2015;45:72–82.
[18] Bartecki A, TÍczaÍ T, Raczko M. The color of transition metal compounds. II. Solvatochromism of Cobalt (II) chloride. Spectrosc Lett 1991;24:559–75.
[19] Abdel-Rahim FM, Mahmoud KH, Aly KA. Optical characterization and differential scanning calorimetry studies of carboxymethyl cellulose-nickel chloride composite system. J Appl Polym Sci 2013;127:4334–9.
[20] Hsiao P-Y, Luijten E. Salt-induced collapse and reexpansion of highly charged flexible polyelectrolytes. Phys Rev Lett 2006;97:148301.
[21] Wei J, Hoagland DA, Zhang G, Su Z. Effect of divalent counterions on polyelectrolyte multilayer properties. Macromolecules 2016;49:1790–7.
[22] Leyssens L, Vinck B, Van Der Straeten C, Wuyts F, Maes L. Cobalt toxicity in humans—A review of the potential sources and systemic health effects. Toxicology 2017;387:43–56.
[23] Poonkothai M, Shyamala Vijayavathi B. Nickel as an essential element and a toxicant. Int J Environ Sci 2012;1:285–8.
[24] Bonaventura R, Zito F, Chiaramonte M, Costa C, Russo R. Nickel toxicity in P. lividus embryos: Dose dependent effects and gene expression analysis. Mar Environ Res 2018;139:113–21.
[25] Moffat I, Martinova N, Seidel C, Thompson CM. Hexavalent Chromium in Drinking Water. J Am Water Works Assoc 2018;110:E22–35.
[26] Anderson RA, Bryden NA, Polansky MM. Lack of toxicity of chromium chloride and chromium picolinate in rats. J Am Coll Nutr 1997;16:273–9.
[27] Jana S, Jana S. Natural polymeric biodegradable nanoblend for macromolecules delivery. In: Visakh PM, Marković G, Pasquini D, editors. Recent Dev. Polym. Macro, Micro Nano Blends. Elsevier; 2017. p. 289–312.
[28] Salles THC, Lombello CB, D'Ávila MA. Electrospinning of gelatine/poly (vinyl pyrrolidone) blends from water/acetic acid solutions. Mater Res 2015;18:509–18.
[29] Coats AW, Redfern JP. Kinetic parameters from thermogravimetric data. Nature 1964;201:68–9.
[30] Yakuphanoglu F, Gorgulu AO, Cukurovali A. An organic semiconductor and conduction mechanism: N-[5-methy1-1,3,4-tiyodiazole-2-yl] ditiyocarbamate compound. Phys B Condens Matter 2004;353:223–9.
[31] Muyonga J, Cole CG, Duodu K. Fourier transform infrared (FTIR) spectroscopic study of acid soluble collagen and gelatine from skins and bones of young and adult Nile perch (Lates niloticus). Food Chem 2004;86:325–32.
[32] Bigi A. Relationship between triple-helix content and mechanical properties of gelatine films. Biomaterials 2004;25:5675–80.
[33] Friess W, Lee G. Basic thermoanalytical studies of insoluble collagen matrices. Biomaterials 1996;17:2289–94.
[34] Djabourov M, Leblond J, Papon P. Gelation of aqueous gelatine solutions. I. Structural investigation. J. Phys. 1988;49:319–32.
[35] Al-Saidi, Al-Alawi, Rahman, Guizani N. Fourier transform infrared (FTIR) spectroscopic study of extracted gelatine from shaari (Lithrinus microdon) skin: effects of extraction conditions. vol. 19. 2012.
[36] Saddeek YB, Azooz MA, Kenawy SH. Constants of elasticity of Li_2O-$B2O_3$-fly ash: Structural study by ultrasonic technique. Mater Chem Phys 2005;94:213–20.
[37] Singh H, Yadav KL. Structural, dielectric, vibrational and magnetic properties of Sm doped $BiFeO_3$ multiferroic ceramics prepared by a rapid liquid phase sintering method. Ceram Int 2015;41:9285–95.
[38] Bartecki A, Tłaczała T. The color of transition metal compounds. I. Trichromaticity colorimetry of aqueous solutions of some Cr(III), Co(II), Ni(II) and Cu(II) compounds. Spectrosc Lett 1990;23:727–39.
[39] Elving PJ, Zemel B. Absorption in the ultraviolet and visible regions of chloroaquochromium(III) ions in acid media. J Am Chem Soc 1957;79:1281–5.
[40] Abd El-Kader FH, Gaafer SA, Abd El-Kader MFH. Characterization and optical studies of 90/10 (wt/wt%) PVA/β-chitin blend irradiated with γ-rays. Spectrochim Acta Part A Mol Biomol Spectrosc 2014;131:564–70.